JOURNAL OF GEOPHYSICAL RESEARCH, VOL. 88, NO. C14, PAGES 9823–9831, NOVEMBER 20, 1983

Measurement of Breaking Waves by a Surface Jump Meter

M. S. LONGUET-HIGGINS AND N. D. SMITH

Institute of Oceanographic Sciences

Quantitative information on the strength and size distribution of whitecaps in a given wave field is very scarce. During the MARSEN field experiments, observations of surface elevation were made with a capacitance wire wave recorder attached to a free floating spar buoy. Automatic analysis of the records with a differentiating circuit and counter allowed a histogram of jump-heights to be constructed corresponding to any preset critical rise rate R of the surface elevation. Over a certain range of R the histogram was nearly independent of the precise value of R. This occurred usually when $0.6 < R/c_0 < 1.0$ where c_0 was the speed of the dominant waves. Records were obtained in wind speeds ranging from 1 to 14 m/s. At 14 m/s the number of "jumps" indicating either steep or breaking waves was of the order of 1 every 100 wave periods. It is shown that this number is consistent with previous theoretical estimates, and with visual observations of whitecap coverage. Because of the dispersive properties of waves, whitecapping in deep water is intermittent. Both theoretical calculation and laboratory experiments lead us to expect steep or breaking waves to induce separated flow, with a high local input of momentum to the wave field. It is concluded that such local events could contribute significantly to the total horizontal stress exerted by the wind.

1. INTRODUCTION

Breaking waves in deep water are intimately involved in a number of processes at the air-sea boundary, including the horizontal stress exerted by wind [*Banner and Melville*, 1976], the generation and dissipation of surface waves, the vertical mixing in the upper ocean, the exchange of heat and gases (enhanced by vertical mixing), and the generation of aerosols by bursting bubbles [*Blanchard and Woodcock*, 1957].

On the other hand, the frequency of occurrence of breaking waves and also their intensity have been little studied. Certain descriptive properties are indeed implicit in the Beaufort wind scale. But the best known quantitative information seems to be in terms of whitecap coverage [see, e.g., *Monahan*, 1971]. Disregarding any possible subjectivity in the visual observations, this still gives only an indirect measure of the dynamical characteristics of the breakers. Moreover, the scatter in the data when plotted against local wind speed suggests strongly that the local wind speed is not the only relevant physical parameter.

There is clearly a need for direct, instrumental measurements of breaking waves to give quantitative information of their physical properties such as the height of the "jump" at the surface, the distribution of whitecap dimensions, and the intensity of the accompanying turbulence. Moreover, these quantities need to be related to the local wave field and to the time history of any relevant winds.

As a first step in this direction, we have (since 1974) tried various methods of measuring breakers in deep water. One method was to record their acoustical signature. However, the main difficulty with (passive) acoustical detection is that the signal depends rather strongly on the distance from the source to receiver; thus under breaking wave conditions only the mean acoustical intensity can be easily interpreted.

We also attempted to calibrate breaking waves by their ability to overturn floating discs of different diameters. On the whole, larger waves overturned larger discs. However, it was found that occasionally the same wave that overturned a large disc would leave unturned a similar disc of smaller diameter. Thus the method apparently was unreliable.

We therefore resorted to the more direct method described in section 2 below, in which the aim was to detect and measure the small jumps or discontinuities in surface elevation associated with spilling or plunging breakers. The instrument designed for this purpose is described in section 3. After successful testing of a model in the 1980-ft (604 m) wave channel at Wormley, the prototype was first deployed from the Nordwijk observation tower off the Dutch coast, as a part of the MARSEN field program (see section 4). An analysis of the results will be given in sections 5 and 6. We also discuss the implication of the results for wind stress and wave generation.

2. PRINCIPLE OF MEASUREMENT

Suppose that the elevation η of the sea surface is measured as a function of time t at an almost fixed horizontal position (x, y), as in Figure 1. A progressive wave passing the recorder will generally show a smooth rate of rise $\partial\eta/\partial t$. But if a breaking wave passes the recorder, we expect a sudden jump in surface elevation. For a plunging breaker (Figure 1*a*) this is relatively large, for a spilling breaker (Figure 1*b*) it is smaller. We remark that spilling breakers may start either as instabilities on the forward face of the wave or as small-scale plunging breakers near the wave crest, which then spread down the forward face [*Longuet-Higgins and Turner*, 1974].

Suppose then that the output voltage $V(t)$ from a capacitance wire recorder is passed through a differentiating circuit, as in Figure 2. When dV/dt exceeds a certain threshold value μ, say, a gate G triggers an integrating circuit I. This integrates the signal dV/dt between the time t, when dV/dt rises through μ until the next instant t_2 when dV/dt falls below μ again. The resulting "jump"

$$J = \int_{t_1}^{t_2} \frac{dV}{dt}\, dt = V(t_2) - V(t_1) \tag{1}$$

is then automatically sorted into a histogram by the counter C, which divides the range of jumps into intervals with preset divisions:

$$0 = J_1, J_2, \cdots, J_m \tag{2}$$

Copyright 1983 by the American Geophysical Union.

Paper number 3C0481.
0148-0227/83/003C-0481$05.00

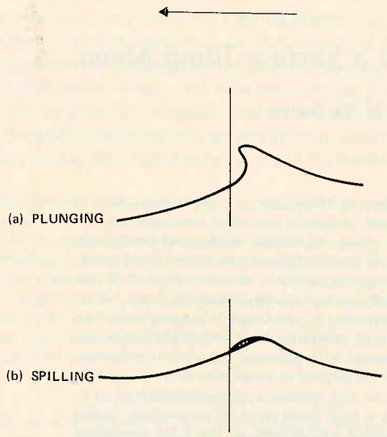

Fig. 1. Illustration of (*a*) a plunging breaker and (*b*) a spilling breaker passing a vertical wire recorder.

It is convenient to make the J_i correspond to integer multiples of a certain jump height $\Delta\mu = \delta$, say.

The resulting histogram depends clearly on the selected values of μ and δ, to an extent which we shall aim to minimize.

3. The Measuring Apparatus

A sketch of the apparatus is shown in Figure 3. The sensing wire is carried on a vertical spar buoy of total length 5.04 m. Buoyancy is provided by two dahn buoys near the center, and angular stability is provided by a weight at the bottom. The total weight is 120 kg. A central hollow tube piercing the water surface gives vertical stability, and a directional fin attached to the central tube keeps the buoy in line either with the current or with the wind, whichever is the stronger. The signal from the sensor is carried by cable to the recording equipment on a ship or stationary platform.

A scale model, of overall length 2.0 m, was first built and tested in the 30-m wave channel at Wormley, in mechanically generated waves of period about 1 s. It was verified that the critical rate of rise $\partial\eta/\partial t = R$ could be set in such a way that the jump-detecting circuit responded only to spilling or plunging breakers and not to steep, nonbreaking waves.

The full-scale apparatus, shown in Figure 4, was first deployed from the Nordwijk observation tower 10 km from the Dutch coast, at 52°16.4′N, 4°17.8′E during the MARSEN field

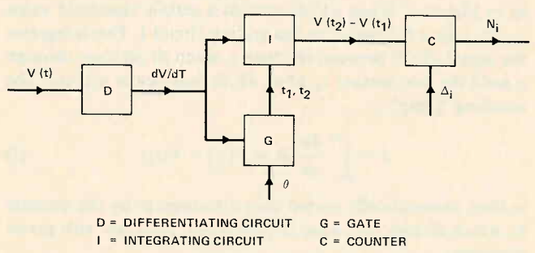

Fig. 2. Block diagram of the circuit for automatic measurement of the histogram of jump heights.

experiment in October-November 1979. For the times of observation see Table 1.

The buoy was launched from a platform on the SE corner of the tower (see Figures 4*a* and 4*b*), and times of observation were restricted to those periods when the tidal currents carried the buoy away from the structure toward the south.

During the first half of the period of observation (September 27 to October 15), preliminary results were obtained, with the critical rate of rise R set arbitrarily. During the remaining period the electrical output $V(t)$ from the capacitance wire was recorded on magnetic tape, so that the output could be rerun later at various settings of μ or, equivalently, R.

4. Analysis of Results

Figure 5 shows a typical length of record taken from run 2 on September 27, 1979. On the trace below can be seen the jumps J as detected by the circuits of Figure 2. The scale of the jump trace is the same as that of the record above.

The way in which the histogram of jump heights J depends on the critical rate of rise R can be seen, in a typical case, in Figure 6. The vertical coordinate N_i represents the total number of jumps, in a 10-min record, which exceed $(i-1)\delta$. Thus the uppermost curve $i = 1$ in Figure 6*a* represents the total number of jumps in the record; the next curve $i = 2$ represents the total number of jumps exceeding δ, and so on. Clearly, as R increases, so N_i decreases monotonically. However, for $i \geq 2$ there is a certain range of R over which each of the curves for N_i is nearly horizontal, in this case 6.5 m/s $< R <$ 9.0 m/s. Over this range the distribution is nearly independent of R.

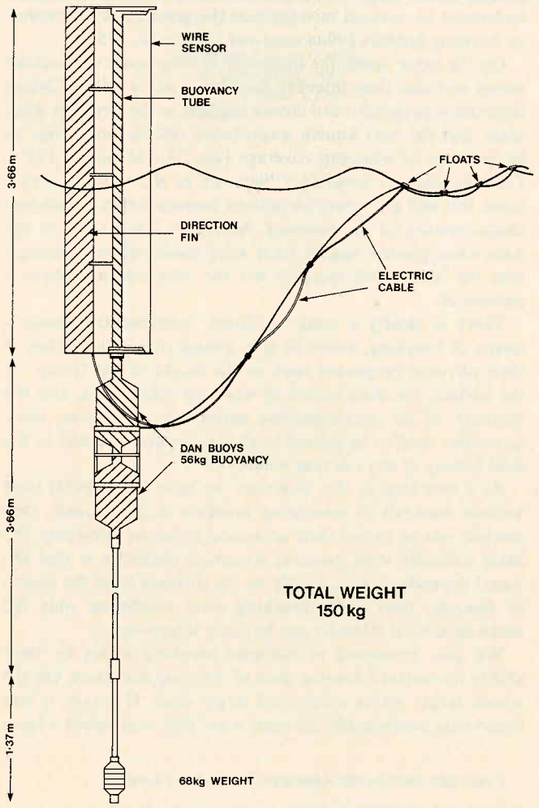

Fig. 3. Sketch of the surface jump meter.

An exception is the curve for $i = 1$, which generally descends more steeply than the others. This curve, which includes jumps of very small amplitude, will clearly be affected by any high-frequency noise, and we shall therefore disregard it.

The corresponding histogram of jump heights is found by taking the differences

$$\Delta N_i = N_i - N_{i-1} \tag{3}$$

at some particular value of R within the chosen range. Figure 6*b* shows the histogram when $R = 8.2$ m/s, for example.

The analysis of other typical records is shown in Figure 7–9. In Figure 9 there is clearly no range of R over which the curves N_i can be considered as horizontal. In such a case we conclude that there are no significant jumps in the record.

Table 2 shows the results from all the records that were analyzed in this way. The given value of R denotes the midpoint, approximately, of the corresponding range.

Also shown in Table 2 is the mean wind speed U, as recorded by an anemometer on the tower, at a height of 20 m above mean sea level; and the phase speed c_0 of the dominant waves in each record, that is, the speed of a regular train of waves, of low amplitude, having the same number of zero crossings as the actual record.

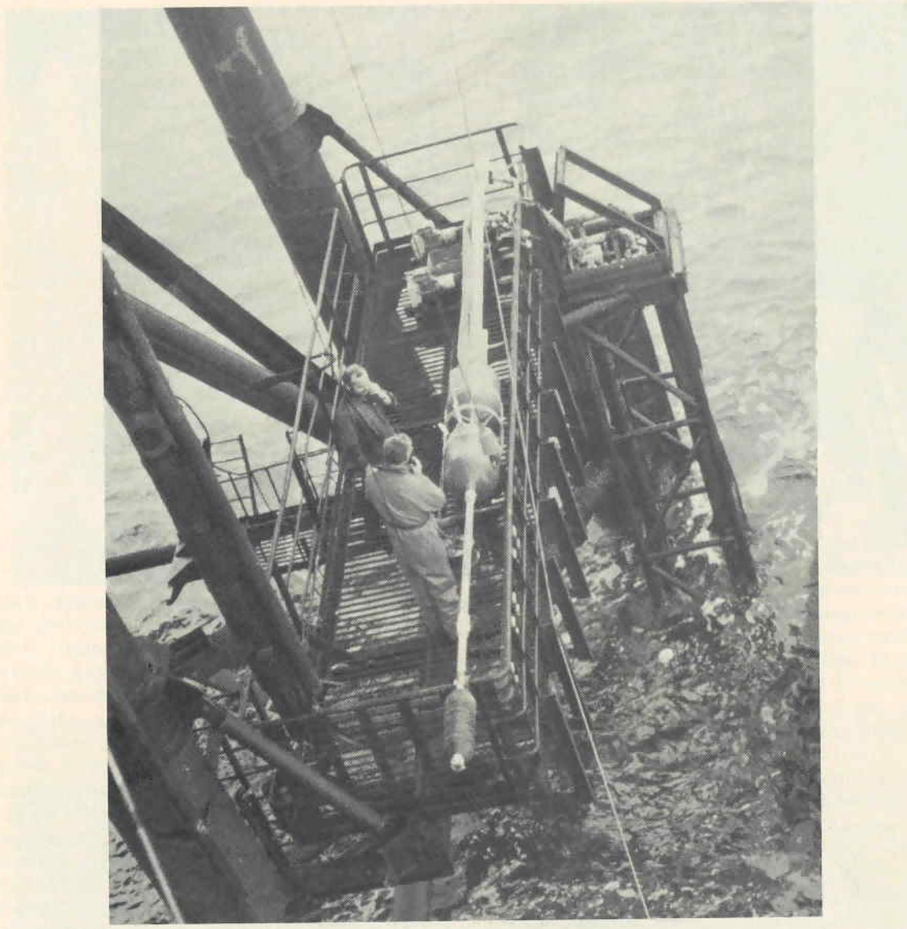

Fig. 4*a*. The buoy in horizontal position before launching.

5. Interpretation

How should we interpret the results of Table 2? Consider first the relation of R to c_0. Figure 10 shows schematically a regular wave progressing to the left. The apparent rate of rise of the surface at a given point is clearly

$$R = \frac{\Delta\eta}{\Delta t} = c\,\frac{\Delta\eta}{\Delta x} \tag{4}$$

where c is the phase speed and $\Delta x = c\Delta t$. But $\Delta\eta/\Delta x = \tan\alpha$, where α is the angle of inclination of the surface to the hori-

Fig. 4*b*. The buoy just after launching, being carried away from the tower by the tidal current.

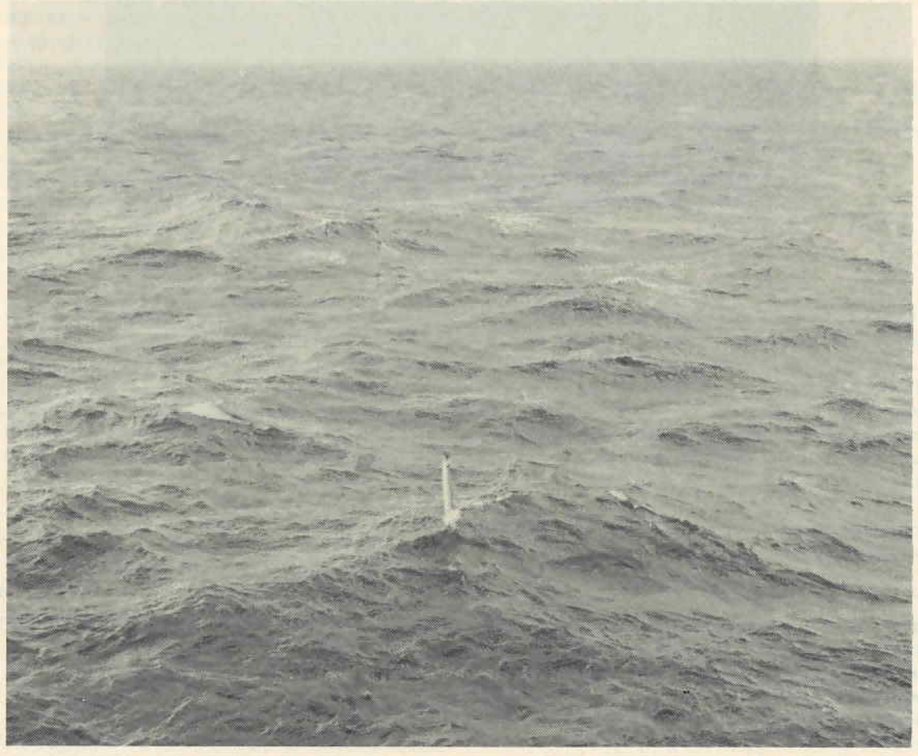

Fig. 4*c*. The buoy in position 60 m from the tower.

TABLE 1. Times of Observation With the IOS Surface Jump Meter From the Nordwijk Platform

Run	Date	Time	Wind Speed, m/s	Wind Direction
2	Sept. 27	1554–1614	8.0	240°
3	Sept. 27	1654–1714	7.5–7.0	240°
4	Sept. 28	1430–1450	4.0	25°
5	Sept. 28	1525–1543	1–2	25°
6	Oct. 4	0830–0850	8.4	165°
7	Oct. 4	0915–0935	8.0–6.4	160°
8	Oct. 18	0920–0940	13.7	300°
9	Oct. 18	1005–1035	13.7	300°
10	Oct. 18	1038–1115	14.2	300°
11	Oct. 19	1015–1100	11.4	220°
14	Nov. 20	1100–1140	6.6	036°
15	Nov. 20	1140–1200	5.2–4.3	039°
16	Nov. 23	1230–1355	10.8	252°
17	Nov. 24	1330–1440	6.7–7.2	220°

zontal. Hence

$$R = c \tan \alpha \tag{5}$$

or

$$\alpha = \arctan (R/c) \tag{6}$$

Now in a regular progressive gravity wave, the maximum inclination of the surface is 30.37° [see *Longuet-Higgins and Fox*, 1977]. Hence the maximum value of R/c is tan 30.37° = 0.586. Any progressive wave in which R/c exceeds this critical value must be breaking. Thus it is interesting that in Table 2 all the ratios R/c_0 lie somewhat above this value.

Our conclusion must be that the jumps registered occur mainly on the forward face of steep, unstable waves. They are not necessarily either white-caps or plunging breakers. Nevertheless, in the absence of a complete knowledge of the local dynamics of steep, progressive but uniform waves, it seems reasonable to suppose that these are mainly waves that are just about to break, it not actually breaking.

Examination of all the plots of N_i versus R showed that in only one case did N_2, N_3, ···, not become zero when $R > c_0$ (that is, when the angle of inclination exceeds 45°). The exception is in Figure 6, for the run from 1005 to 1015 on October 18. This shows a single occurrence of what may have been a plunging breaker actually striking the spar buoy. In the remaining cases we may suppose that the waves were on the point of breaking.

The question of the phase of the jumps relative to that of the corresponding wave must also be examined. It seems that in every case the jumps occurred on the forward face of the wave, that is ahead of the crest, as seen on the record. Some allowance must be made for the phase shift in the response of the buoy. The appendix gives a simplified theoretical analysis. From Figure 12*b* it appears that generally the total phase-lag $(\phi_A + \phi_B)$ is negative. This implies that the phase of the response leads the phase of the surface elevation. At high frequencies the total phase lag tends to zero, so high-frequency "jumps" are registered without appreciable time lag, but their occurrence is delayed relative to a longer wave. In other words a "jump" is further down the forward face of the wave than appears on the record. However, the total phase shift $|\phi_A + \phi_B|$ is not large, being less than 30° for waves of period 7 s or less (corresponding to phase speeds c_0 of less than 11 m/s).

6. DISCUSSION

The last column of Table 2 indicates that under the given range of conditions the number N of apparently breaking waves in a 10-min record was typically between 0 and 8.

Is this result reasonable in terms of present knowledge?

Let ϖ denote the proportion of dominant waves that have whitecaps. Table 2 indicates that on October 18, for example, the wave period was around 6.0 s, so that the number of waves in 10 min was about 100. With $N = 3$ this gives $\varpi = 3 \times 10^{-2}$, which is within the range calculated theoretically by *Longuet-Higgins* [1969].

Again, if the foam from a typical "jump" has a persistence time T_p, then the proportion of the sea surface covered by foam (the visual whitecap coverage (VWC) will be

$$\text{VWC} = \varpi T_p / T \tag{7}$$

where T is the wave period. For salt water, *Monahan and Zietlow* [1969] found $T_p = 3.85$ s; whence VWC $\doteqdot 2 \times 10^{-2}$. This value lies well within the range of observations reported by *Monahan* [1971, Figure 2] for a wind of 14 m/s.

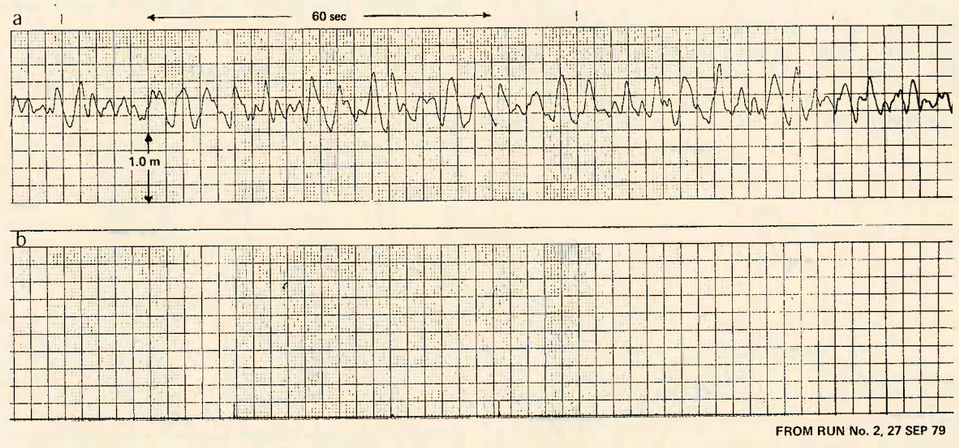

Fig. 5. (*a*) A typical length of record taken from run 2 on September 27, 1979. (*b*) The corresponding trace of jumps.

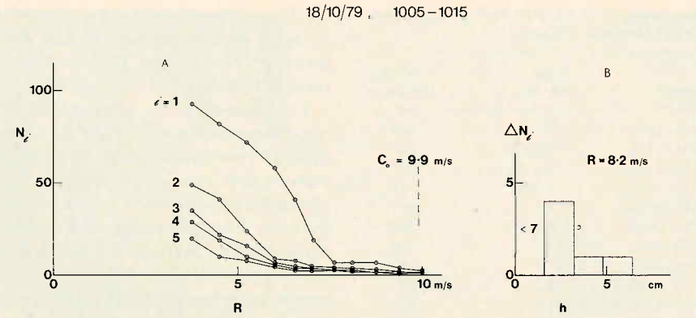

Fig. 6. (*a*) The number N_i of jumps of magnitude h between $(i-1)\delta$ and $i\delta$, as a function of the critical rate of rise R, during the 10-min interval 1005–1015 (local time) on October 18. (*b*) The corresponding histogram of jump heights; $\delta = 0.32$ cm.

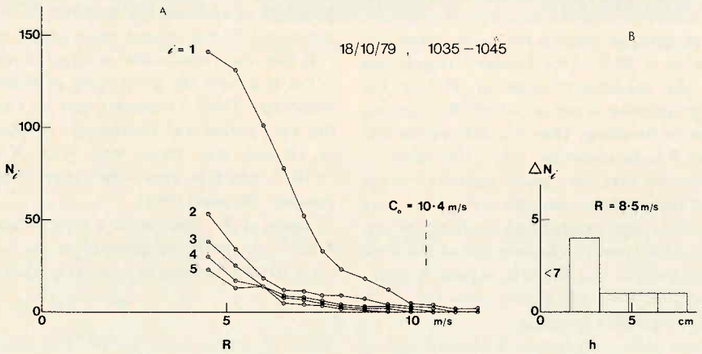

Fig. 7. As in Figure 6, for the interval 1035–1045 on October 18.

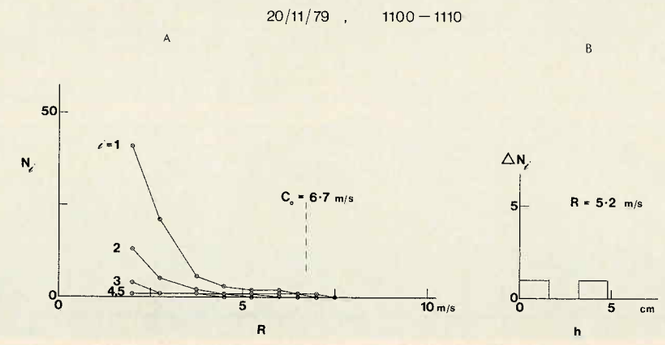

Fig. 8. As in Figure 6, for the interval 1100–1110 on November 20.

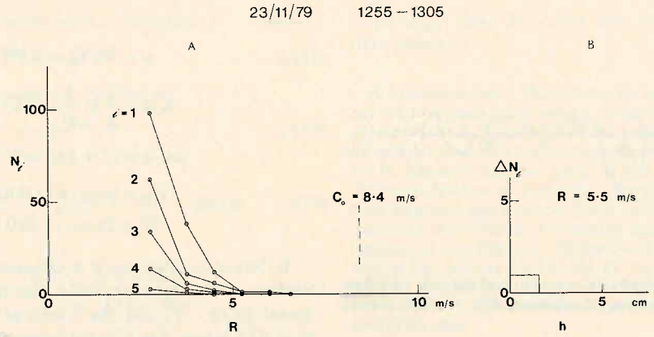

Fig. 9. As in Figure 6, for the interval 1320–1330 on November 23.

In spite of the preliminary nature of the observations it may be interesting to discuss the possible implications of this result for two aspects of air-sea interaction: the horizontal stress exerted by the wind and the input of energy to the waves.

Horizontal stress. It was shown very clearly by *Banner and Melville* [1976] that the occurrence of whitecaps and short breaking waves near the crest of a steep gravity wave tended inevitably to induce a separation of the airflow over the wave. Measurements indicated that the flux of horizontal momentum from the air to the water was thereby increased locally by a factor of order 50. Though occasional separation of the airflow may also occur when the waves are not breaking, nevertheless, it seems probable that breaking waves induce separation far more strongly and consistently.

Two questions then arise: How frequently are breaking waves observed in the ocean, and what proportion of the total wind stress can the local patches of breaking be expected to account for?

With regard to the first question we note first that wave breaking is an essentially intermittent phenomenon, especially in deep water. This is due to the fact that surface waves are both dispersive and irregular; high waves occur in groups, with individual waves traveling through the group at a speed c which is greater than the group velocity c_g. Thus a wave will start at the rear of a group, grow to its maximum steepness as it passes through the group, and die away as it reaches the front of the group. A whitecap will be seen only momentarily when the wave is near its point of maximum steepness. Since the speed of the wave relative to its envelope is $(c - c_g)$ or about $\frac{1}{2}c$, whitecaps are seen intermittently, with a frequency about half that of the waves themselves [see *Donelan et. al.*, 1972].

The separation of the airflow must therefore be intermittent also. No precisely appropriate calculations of the airflow are available, and it is reasonable to compare the onset of separation with some recent calculations of the flow started from rest over a steep but regular train of waves [*Longuet-Higgins*, 1980]. The variation of the drag coefficient c_D with time is shown in Figure 11; c_D begins at $t = 0$ with a relatively high value of 0.15 due to the formation of a circulating eddy behind each crest. Once the eddy is formed, however, the momentum of the airflow changes less rapidly, and the drag coefficient falls drastically to a level whose mean is far less, by perhaps two orders of magnitude. The high drag is thus a momentary phenomenon, lasting for a time T_D of order $L/(U-c)$, where L is the wavelength and U the wind speed. Since the wave period T is equal to L/c, it follows that

$$T_D/T \doteq c/(U-c) \tag{8}$$

which, in the case of the data of Table 2, is of order 1 at least. The contribution of steep waves to the total mean drag coefficient is then of order

$$c_D' = \varpi c_{D0}(U-c)^2/c^2 \tag{9}$$

where c_{D0} denotes the initial drag coefficient for the high waves. Conservatively, we may take, from Figure 11, $c_{D0} \doteq 0.075$. In table 2, for the data of October 18, $(U-c)/c$ is of order 0.3, giving $c_D' \doteq 0.6 \times 10^{-3}$. This is smaller than the customary coefficient $c_D \doteq 1.5 \times 10^{-3}$, but nevertheless of the same order of magnitude.

TABLE 2. Analysis of Data

Date	Time	U, m/s	c_0 m/s	R, m/s	N
Oct. 18, 1979	0922–0932	13.7	7.6	6.5	3
Oct. 18, 1979	0935–0945	13.7	9.2	8.0	1
Oct. 18, 1979	1005–1015	13.7	9.9	8.2	6
Oct. 18, 1979	1035–1045	14.2	10.4	8.5	7
Oct. 18, 1979	1055–1105	14.2	10.6	8.5	5
Oct. 19, 1979	1020–1030	14.4	9.5	—	0
Oct. 19, 1979	1051–1101	14.4	7.9	6.5	5
Nov. 20, 1979	1100–1110	6.6	6.7	5.0	2
Nov. 20, 1979	1130–1140	5.2	5.2	—	0
Nov. 23, 1979	1230–1240	10.8*	8.4	5.5	1
Nov. 23, 1979	1255–1305	10.8*	8.4	5.5	1
Nov. 23, 1979	1320–1330	10.8*	8.4	—	0
Nov. 24, 1979	1335–1345	6.7	6.6	5.0	2
Nov. 24, 1979	1412–1422	6.9	6.7	5.0	2

*Heavy rain.

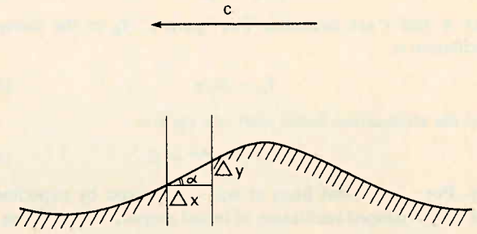

Fig. 10. Interpretation of the rate of rise R for a progressive wave.

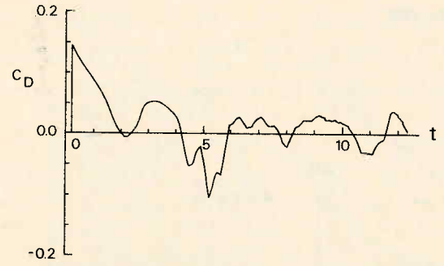

Fig. 11. The drag coefficient c_D as a function of the time t for flow over a sharp-crested wave form of steepness $H/L = 0.169$, started from rest at time $t = 0$.

Equation (9) suggests also that for the same values of ϖ and c_{D0}, the contribution c_D' will be a strongly increasing function of U/c. This is in agreement with the ideas and observations expressed by *Longuet-Higgins* [1969] and *Kitaigorodskii* [1973, p. 88]. (There is also experimental evidence from the analysis of storm surges from hurricanes that the effective drag coefficient should be increased at high values of U/c [see *Whitaker et al.*, 1975].)

We conclude that flow separation induced by steep waves could well make a significant contribution to the mean horizontal wind stress.

APPENDIX: RESPONSE OF A SPAR BUOY
A SIMPLIFIED THEORY

Theoretically, the vertical displacement y of the buoy from its equilibrium position may be assumed to be governed by the equation

$$\ddot{y} + C|\dot{y}|\dot{y} + \omega_0{}^2 y = 0 \tag{A1}$$

in free motion, where C is a drag coefficient per unit mass, and ω_0 is the natural (radian) frequency of oscillation. It is convenient to replace the damping term by a linear expression $K\dot{y}$, with K chosen so that total dissipation over one cycle is the same, that is,

$$\int K\dot{y}^2\, dt = \int C|\dot{y}|^3\, dt \tag{A2}$$

Thus K, though a constant, depends in fact on the amplitude of the oscillation. The resulting equation of free oscillation is

$$\ddot{y} + K\dot{y} + \omega_0{}^2 y = 0 \tag{A3}$$

When $K < 2\omega_0$, this has solutions of the form

$$y = Ae^{-Kt/2}\cos(\alpha t + \varepsilon) \tag{A4}$$

where

$$\alpha = (\omega_0{}^2 - \tfrac{1}{4}K^2)^{1/2} \tag{A5}$$

and A and ε are constant. The "period" T_D of the damped oscillation is

$$T_D = 2\pi/\alpha \tag{A6}$$

and the attenuation factor over one cycle is

$$e^{-KT_D/2} = e^{-\pi K/\alpha} = D \tag{A7}$$

say. For the present buoy it was determined by experiment that for a damped oscillation of initial amplitude $A = 1.0$ m,

$$T_D = 10.5 \text{ s} \qquad D = 0.14 \tag{A8}$$

Hence

$$\alpha = 2\pi/T_D = 0.598 \text{ rad/s}$$

$$K/\alpha = \frac{1}{\pi}\ln\frac{1}{D} = 0.63$$

$$\omega_0/\alpha = (1 + \tfrac{1}{4}K^2/\alpha^2)^{1/2} = 1.048 \tag{A9}$$

$$\omega_0 = \alpha(\omega_0/\alpha) = 0.627 \text{ rad/s}$$

$$T_0 = 2\pi/\omega_0 = 10.0 \text{ s}$$

In forced oscillations, if Y denotes the elevation of the free surface above its mean value, the restoring force is proportional to $(y - Y)$ and the frictional force is proportional to $(\dot{y} - \beta\dot{Y})$, where β is a factor depending on the depth d of the main source of friction (in our case the buoyancy chambers) below the surface. In deep water we expect that

$$\beta = e^{-kd} = e^{-\omega^2 d/g} \tag{A10}$$

where k is the wave number and ω the radian frequency of the waves. When d is small compared to the wavelength $L = 2\pi/k$, then β is nearly equal to 1. But if $d > 0.25L$, then β is small. From (A3) it can be seen that the (linearized) equation governing the motion must in general be

$$\ddot{y} + K(\dot{y} - \beta\dot{Y}) + \omega_0{}^2(y - Y) = 0 \tag{A11}$$

But the signal $V(t)$ recorded by the spar buoy is proportional to $(Y - y) = \eta$, say. From (A11), writing $y = Y - \eta$, we have for η the equation

$$\ddot{\eta} + K\dot{\eta} + \omega_0{}^2\eta = \ddot{Y} + K(1 - \beta)\dot{Y} \tag{A12}$$

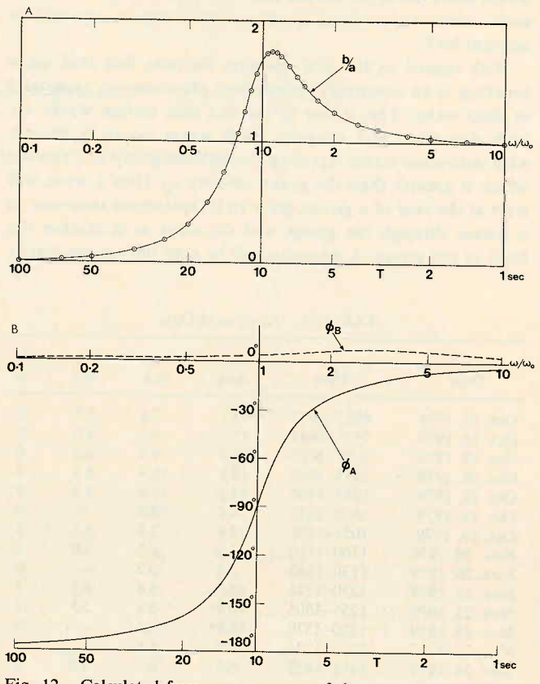

Fig. 12. Calculated frequency response of the spar buoy and jump meter (*a*) amplitude and (*b*) phase lag $\phi = \phi_A + \phi_B$.

Hence the response to the sinusoidal oscillation

$$Y = ae^{i\omega t} \tag{A13}$$

where a and ω are real constants, is given by

$$\eta = be^{i(\omega t - \phi)} \tag{A14}$$

provided

$$(-\omega^2 + iK\omega + \omega_0{}^2)be^{-i\phi} = [-\omega^2 + iK(1 - \beta)\omega]a \tag{A15}$$

so

$$(a/b)e^{i\phi} = \frac{(\omega_0{}^2 - \omega^2) + iK\omega}{-\omega^2 + iK(1 - \beta)\omega} \tag{A16}$$

and the phase lag ϕ will be given by

$$\phi = \arctan\frac{K\omega}{\omega_0{}^2 - \omega^2} + \arctan\frac{K(1 - \beta)}{\omega} \tag{A17}$$

The behavior of ϕ can be seen qualitatively from Figure 12*b*. For very high frequencies, as $\omega/\omega_0 \to \infty$, the argument of both the numerator and denominator in (A16) tends to 180°, so $\phi \to 0°$. That is, for sudden discontinuities or "jumps", η is in-phase with Y (as we would expect). When $\omega > \omega_0$, ϕ lies between 0° and −90°, so η leads the surface elevation Y. When $\omega < \omega_0$, ϕ lies between −90° and −180°, as shown in Figure 12*b*. Finally, as $\omega \to 0$, (A10) shows that $(1 - \beta)$ is of order ω^2, hence $\phi \to -180°$. So for very long waves, η is 180° out of phase with Y.

For calculation it is convenient to write (A17) as

$$\phi = \phi_A + \phi_B \tag{A18}$$

where

$$\phi_A = \arctan\frac{(K/\omega_0)(\omega/\omega_0)}{1 - \omega^2/\omega_0{}^2}$$

$$\phi_B = \arctan\frac{(K/\omega_0)(1 - e^{-\lambda\omega^2/\omega_0{}^2})}{\omega/\omega_0} \tag{A19}$$

and

$$\lambda = d\omega_0{}^2/g \tag{A20}$$

From Figure 3 we may take $d = 3$ m, and then from (A9) we find $\lambda = 0.120°$. Also

$$K/\omega_0 = (K/\alpha)/(\omega_0/\alpha) = 0.60 \tag{A21}$$

The angles ϕ_A and ϕ_B are shown in Figure 12*b*. Clearly, ϕ_B is quite small (less than 7°) and the main contribution comes from ϕ_A. The "resonant" period T_0 in this case is 10.0 s. Phase shifts larger than 30° occur only for wave periods T greater than about 7 s.

Acknowledgments. The authors are much indebted to B. McCartney for assistance in the design of the electronic circuits used in the apparatus, to R. Spanhoff and his colleagues at the Rijkswaterstaat for collaboration and logistic support on the Nordwijk tower, and to O. H. Shemdin and his group at the Jet Propulsion Laboratory, California Institute of Technology, for allowing us to use channels on their magnetic tape recorder. Their work was carried out under contract with the National Aeronautics and Space Administration. This manuscript was begun in England and completed during a visit by one of the authors (M.S.L.-H.) to the Department of Engineering Sciences at the University of Florida, Gainesville, Florida, during February 1981. Comments and discussions were provided by members of his class.

REFERENCES

Banner, M. L., and W. K. Melville, On the separation of air flow over water waves, *J. Fluid Mech.*, *77*, 825–842, 1976.

Blanchard, D. C., and A. H. Woodcock, Bubble formation and modification in the sea and its meteorological significance, *Tellus*, *9*, 145–158, 1957.

Donelan, M., M. S. Longuet-Higgins, and J. S. Tunner, Periodicity in whitecaps, *Nature*, *239*, 449–451, 1972.

Kitaigorodskii, S. A., *The Physics of Air-Sea Interaction*, translated from the Russian by A. Baruch, 237 pp., Israel Program for Scientific Translations, Jerusalem, 1973.

Longuet-Higgins, M. S., On wave breaking and the equilibrium spectrum of wind-generated waves, *Proc. R. Soc. London Ser. A*, *310*, 151–159, 1969.

Longuet-Higgins, M. S., Polygon transformations in fluid mechanics, in *Proceedings of the 7th International Conference on Numerical Methods in Fluid Dynamics, Stanford, California, June 23–24, 1980*, Springer, Berlin, 1980.

Longuet-Higgins, M. S., and M. H. Fox, Theory of the almost-highest wave: The inner solution, *J. Fluid Mech.*, *80*, 721–741, 1977.

Longuet-Higgins, M. S., and J. S. Turner, An "entraining plume" model of a splilling breaker, *J. Fluid Mech.*, *63*, 1–20, 1974.

Monahan, E. C., Oceanic whitecaps, *J. Phys. Oceanogr.*, *1*, 139–144, 1971.

Monahan, E. C., and C. R. Zietlow, Laboratory comparisons of freshwater and salt-water whitecaps, *J. Geophys. Res.*, *74*, 6961–6966, 1969.

Nath, J. J., and F. L. Ramsey, Probability distributions of breaking wave heights emphasizing the utilization of the JONSWAP spectrum, *J. Phys. Oceanogr.*, *6*, 316–323, 1976.

Whitaker, R. E., R. O. Reid, and A. C. Vastano, An analysis of drag coefficient at hurricane windspeeds, *Tech. Memo 56*, Coastal Eng. Res. Cent., Fort Belvoir, Va., 1975.

M. S. Longuet-Higgins and N. D. Smith, Institute of Oceanographic Sciences, Wormley, Surrey, England.

(Received August 17, 1982;
accepted March 21, 1983.)